INTERNATIONAL JOURNAL OF COMPUTERS COMMUNICATIONS & CONTROL
Online ISSN 1841-9844, ISSN-L 1841-9836, Volume: 19, Issue: 4, Month: August, Year: 2024
Article Number: 6608, https://doi.org/10.15837/ijccc.2024.4.6608

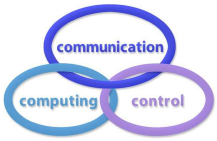

CCC Publications

Fault Diagnosis and Localization of Transmission Lines Based on R-Net Algorithm Optimized by Feature Pyramid Network

C.M. Zhang, X.Q. Xu, S.L. Liu,Y.J. Li,J.F. Jiang

Chunmei Zhang*
Guangdong Power Grid Co., Ltd.
Zhongshan Power Supply Bureau
Zhongshan, Guangdong, 528400, China
*Corresponding author: swkj01@126.com

Xingque Xu
Guangdong Power Grid Co., Ltd.
Zhongshan Power Supply Bureau
Zhongshan, Guangdong, 528400, China
xuxingque@zs.gd.csg.cn

Silin Liu
Guangdong Power Grid Co., Ltd.
Zhongshan Power Supply Bureau
Zhongshan, Guangdong, 528400, China
liusilin0808@zs.gd.csg.cn

Yongjian Li
Guangdong Power Grid Co., Ltd.
Zhongshan Power Supply Bureau
Zhongshan, Guangdong, 528400, China
liyongjian1114@zs.gd.csg.cn

Jiefeng Jiang
Guangdong Power Grid Co., Ltd.
Zhongshan Power Supply Bureau
Zhongshan, Guangdong, 528400, China
jiangjiefeng@zs.gd.csg.cn

Abstract

Timely fault diagnosis and localization of transmission lines is crucial for ensuring the reliable operation of increasingly complex power systems. This study proposes an optimized R-Net algorithm based on a feature pyramid network (FPN) and densely connected convolutional network (D-Net) for transmission line fault diagnosis and localization. The R-Net network is enhanced by reshaping the anchor points using an improved K-means algorithm and incorporating an FPN for multi-scale feature extraction. The backbone network is further optimized using D-Net to strengthen inter-layer

connections and improve feature reuse. Experimental results demonstrate that the optimized R-Net achieves an overall average accuracy of 0.64, outperforming the original network by 1.30%. The accuracy improvement is particularly significant for ground wire defects (2.40%). The D-Net-based R-Net, despite having fewer parameters, maintains high accuracy (0.6502). Compared to other object detection algorithms, such as YOLO-v3 and Faster R-CNN, the optimized R-Net exhibits superior performance in terms of mean average precision (15.58% and 2.45% higher, respectively) and parameter efficiency (17M vs. 38M and 81M). Considering both performance and speed, the optimized R-Net achieves a processing rate of 10.5 frames per second. This study provides an efficient and accurate tool for transmission line fault diagnosis and localization, with significant practical implications for power system operation and maintenance.

Keywords: Deep learning; Transmission lines; Fault; Convolutional neural network; Feature pyramid network.

1 Introduction

Transmission lines are the primary means of power transmission in modern power grid systems. Their safe and stable operation is crucial for the entire power system. Common faults in transmission lines include short circuits, open circuits, insulator faults, and cable connection faults. These faults may lead to power transmission interruption, leakage, or breakdown, thereby affecting the reliability and safety of power supply. However, due to long-term exposure to the external environment, transmission line components are often affected by various factors, such as weather erosion, mechanical stress, etc. These may lead to component damage or functional decline, thereby bringing potential operational risks. To timely detect and address these issues, transmission lines need to be regularly inspected and fault diagnosed [1, 2, 3]. Traditionally, these inspection tasks mainly rely on manual labor. However, this method is not only inefficient, but may also pose security risks. With the advancement of technology, especially drone technology and computer vision, they are gradually being applied to various types of fault diagnosis. Drones equipped with high-definition cameras and combined with deep learning technology for automated inspection and fault diagnosis can not only greatly improve inspection efficiency but also reduce errors caused by human factors [4, 5, 6]. Automatic fault diagnosis using deep learning can effectively overcome the limitations of manual inspection methods and automatically extract and analyze features. This can help improve equipment reliability and production efficiency in industrial production. It is estimated that equipment failures causing production shutdowns result in billions of dollars in losses worldwide every year. However, the current deep learning object detection algorithms still have some limitations in the application of transmission line fault diagnosis, especially in identifying small faults in complex backgrounds. For instance, actual transmission lines may have complex background interferences, such as trees, buildings, and towers. Additionally, minor faults, like damaged insulators and wires, are often imperceptible in images, making it difficult for deep learning object detection algorithms to accurately identify and locate the fault point. Therefore, a transmission line fault diagnosis and localization algorithm based on an improved R-Net has been proposed.

The aim of this study is to enhance current object detection algorithms and improve the performance of models for diagnosing and locating faults in transmission lines. Specifically, the focus is on accurately and stably identifying small faults in complex backgrounds to better suit real-world transmission line scenarios. The research's primary contribution is enhancing the maintenance speed and accuracy of transmission line equipment, shortening fault handling time, and providing more efficient technical support for health monitoring and fault handling of transmission line equipment. Additionally, it improves the application of object detection algorithms in the power systems field. The study's innovation lies in combining feature pyramid network (FPN) and densely connected convolutional network (D-Net) to optimize R-Net and improve its detection accuracy. The research structure is divided into four main parts. The text summarizes the research achievements and shortcomings of deep learning and transmission lines both domestically and internationally. It introduces object detection algorithms and discusses their improvements. The text also includes experiments and analysis of the improved algorithm, comparing it in detail with traditional algorithms. Finally, the text summarizes the experimental results, identifies research shortcomings, and proposes future research directions.

2 Related works

With the rapid and rigorous development of smart grids and power structures, efficient fault detection methods have become the key to ensuring system anti-interference and reducing maintenance costs. Among them, transmission lines play a crucial role. Deep learning is closely related to the detection and diagnosis of transmission line defects[7]. Some scholars have conducted relevant research. Tong et al. proposed a fault detection method for transmission lines based on graph convolutional neural networks (CNNs). This method combined spatial information and powerful feature extraction to establish a detection and classification framework. Based on the adjacency matrix of the topology and voltage signal, this method quickly provided prediction results. The experimental results showed that this method was more effective than existing methods, with high speed, robustness, and strong generalization ability. It was suitable for online transmission line protection [8]. Athamneh et al. proposed a new fault diagnosis method for distance protection of transmission lines, which only used real-time voltage signals. This method combined CNNs and high-order spectral estimation for deep learning classification. A two-dimensional CNN model was developed. The short time Fourier transform of the signal was used to achieve high-precision fault detection. The results indicated that this method had high numerical performance and consistency [9]. Tan et al. proposed a insulator automatic detection technology based on deep learning. A single multi-box detector network was utilized to locate insulators in aerial images and enhance classification functionality. To address the data shortage, data expansion techniques were adopted, including image combination, affine transformation, and brightness adjustment. The experimental results demonstrated the robustness and accuracy of this method in insulator detection [10]. To ensure the reliability and elasticity of electrical energy, rapid and accurate fault detection tools were crucial. Considering the high cost of faults, there was an urgent need to adopt intelligent detection methods, especially powerful machine learning methods. Therefore, Mohammadi et al. delved into various machine learning techniques, such as random forests, support vector machines, and CNNs. They were widely applied in fault detection and classification of transmission lines [11].

Shakiba et al. proposed a transfer learning strategy based on CNNs. By transferring knowledge from the source network, fast and effective fault diagnosis for different transmission lines was realized. Even in the absence of a large amount of label data, this method also outperformed traditional methods. The robustness of this method in various fault scenarios was investigated using seven different datasets, further confirming the reliability in transmission line fault detection [12]. Azizi et al. proposed a transfer learning strategy based on pre trained VGG-19, aimed at detecting transmission line faults in aerial images. By fine-tuning some layers, the new deep CNN successfully distinguished between damaged and intact insulators. In image testing in various environments, this method demonstrated higher superiority compared to other existing methods [13]. Qiu et al. proposed a method for detecting birds that pose a threat to transmission lines. The method combined lightweight CNNs and used 20 bird image datasets related to transmission line faults. The YOLOv4 tiny model was used for training and after adopting various optimization strategies, an average accuracy of 92.04% was achieved on the test set. The comparison with other algorithms verified the efficiency of this method [14]. Gao et al. proposed a power tower anomaly detection system that combined computer vision and the Internet of Things. Sensors that could monitor the status of power towers were designed and drones were used to collect images in case of abnormalities. Cascaded CNNs were used for image analysis, achieving high average accuracy. This scheme had significant value for automatic detection of large-scale power lines[15].

In summary, many cutting-edge experts and scholars at home and abroad have conducted in-depth research and exploration on transmission line fault diagnosis technology. However, there are still some limitations and challenges in practical applications. To this end, a diagnosis and localization method based on the deep learning is proposed to efficiently detect and diagnose faults in transmission lines. This method has a positive promoting effect on the stable development of the power industry and the improvement of diagnostic efficiency.

3 Research method

An improved object detection algorithm is proposed for transmission line defect fault detection. Firstly, CNN is applied to identify defects and faults in transmission lines. Secondly, to more accurately identify small changes, an optimized K-means algorithm is used to reshape the size and quantity of anchor points to adapt to the types of actual transmission line defects and faults. Finally, a FPN in R-Net is established.

3.1 CNN and Fault Identification of Transmission Line Defects

With the rise of deep learning technology, the innovation of CNN has brought a leap in accuracy and speed for defect and fault detection. In the deep learning, CNN has become an indispensable tool in computer vision tasks. The position is becoming increasingly important. In fault recognition using CNN, the features of the input data are extracted by the convolutional layer through the convolutional operation of the filter. The pooling layer reduces the spatial dimension of the feature mapping, the number of parameters, and enhances the model's robustness. The fully connected layer unfolds the feature maps extracted through the convolutional and pooling layers into one-dimensional vectors and classifies them through neural networks. Compared with traditional neural networks, CNN optimizes feature extraction through specific connection methods, reducing computational complexity. The core convolution step captures key information of the image and then upgrades it to advanced semantics. The selection of convolutional kernels is crucial [16, 17]. The relevant convolution calculation is shown in equation (1).

$$h_{W,b}(x) = f(\sum_{j=0}^{J-1}\sum_{i=0}^{I-1} W_{ij}x_{m+i,n+j} + b), (0 \le m \le M, 0 \le n \le N) \tag{1}$$

In equation (1), $h_{W,b}(x)$ represents convolutional output. f represents the activation function. x represents the input. W_{ij} is the convolutional kernel. b is the bias term. Feature maps are generated after image convolution. To simplify information, the feature map area is fused according to algorithms, converting advanced features into basic features, accelerating processing speed, and highlighting the core features of the image. Figure 1 shows examples of maximum and average pooling.

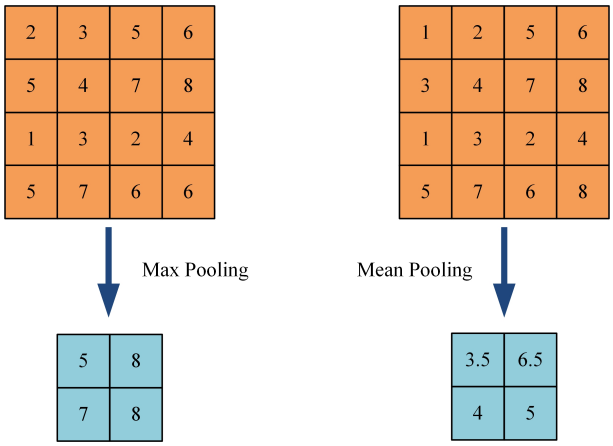

Figure 1: Examples of maximum and average pooling

The neural network includes a fully connected layer in addition to the convolutional and pooling layers to integrate features. This layer connects each node in the feature map to its respective nodes. The activation function maps the output to a specific range, reducing the impact of input changes due to the fluctuation of CNN output. Furthermore, pure linear CNNs are unable to handle complex problems. The activation functions are used to correct nonlinear outputs. Commonly used activation functions include Sigmaid, Tanh, and ReLU. Sigmaid converts real numbers to values of 0-1, as shown in equation (2).

$$S(x) = \frac{1}{1 + e^{-x}} \tag{2}$$

The hyperbolic tangent function Tanh has a similar curve to equation (2), but the tanh center is at 0 and the range is -1 to 1. Tanh maintains a large gradient over a large range, which is less likely to cause the gradient to disappear, making it more practical. The tanh is shown in equation (3).

$$S(x) = \frac{e^{x} - e^{-x}}{e^{x} + e^{-x}} \tag{3}$$

ReLU, also known as the slope function, is currently the most commonly used activation function. It frequently appears in many network structures. The definition is shown in equation (4).

$$f(x) = max(0, x) \tag{4}$$

Although ReLU is widely used, when the learning rate is too high, it may cause neurons to no longer activate. Therefore, corresponding improvement method is proposed. Among them, Leaky-ReLU is negative and assigned a small non zero slope. The loss function, also known as the cost function, is a key indicator for evaluating the deviation between network output and expected results. It plays a core role in model learning and optimization. Mean-square error (MSE) is a common evaluation method. The reduction reflects the progress of model learning. The definition of MSE is shown in equation (5).

$$L(y, \hat{y}) = \frac{(y, \hat{y})^2}{2} \tag{5}$$

Detection techniques often use the cross entropy (CE) function as the evaluation criterion, as shown in equation (6).

$$L(y, \hat{y}) = -\left[y \log \hat{y} + (1 - y) \log (1 - \hat{y})\right] \tag{6}$$

The detection network using convolutional techniques needs to evaluate the output accuracy. In the best case, the correct category output is 1, and the rest is 0. CE loss helps to measure the closeness of network output and overcomes the disadvantage of slow learning speed in MSE. When training a large number of samples, the loss is often the average of the CE function for all samples, as shown in equation (7).

$$J(w, b) = -\frac{1}{m} \sum_{i=1}^{m} \left[y_i \log \hat{y} + (1 - y) \log (1 - \hat{y})\right] \tag{7}$$

3.2 Improved R-Net Algorithm Based on Feature Pyramid Network Model

Some minor deviations or slight shaking of components may be missed. Remote detection may lose some information. Therefore, the recognition accuracy of small changes needs to be further improved. The R-Net is introduced. R-Net uses FPN to integrate image features and achieve multi-scale prediction. A specific loss function is constructed to solve the class imbalance and achieve high accuracy in small target detection. Traditional single-scale feature extraction networks may not be able to fully extract features at different scales, resulting in poor object detection performance at small or large scales. To solve this multi-scale problem in object detection, FPN introduces multi-scale feature layers in the network, thereby improving the performance of object detection. The receptive field (RF) describes the mapping range of feature images on the original image. The central pixel has the greatest impact on the output. In Figure 2, the input feature mapping of 5×5 is obtained through two 3×3-convolutions.

To estimate the receptive region characteristics of each CNN layer, the number of features in each dimension is first calculated. Meanwhile, the details of each layer are also tracked, including the spacing between features, the size of the receptive region, and the starting position of the upper left feature center. The obtained feature mapping expression is shown in equation (8).

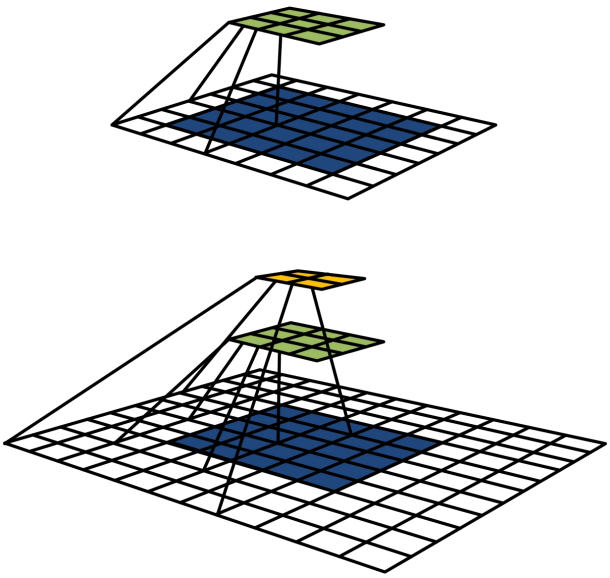

Figure 2: Receptive field diagram

$$n_{out} = \left[\frac{n_{in} + 2p - k}{s}\right] + 1 \tag{8}$$

In equation (8), p represents the filling amount. s represents convolutional step. n represents the receptive area for input feature mapping. k is the scale of the convolutional kernel. j_{out} is the spacing of the output feature mapping. j_{in} represents the spacing of the input mapping. j_{out} is based on j_{in} , as shown in equation (9).

$$j_{out} = j_{in}s \tag{9}$$

r_{out} represents the receptive region of the output feature map. r_{in} is the receptive region of the input mapping. The value of r_{out} is determined based on r_{in} , as shown in equation (10).

$$r_{out} = r_{in} + (k-1)j_{in} \tag{10}$$

$start_{out}$ represents the center position of the first receptive region in the output feature map. The calculation method is shown in equation (11).

$$start_{out} = start_{in} + (\frac{k-1}{2} - p)j_{in} \tag{11}$$

In equation (11), $start_{out}$ represents the first receptive region center of the input feature. In convolutional networks, shallow features have accurate localization, while deep features have rich information but rough localization. Pyramid structures are often used to combine the advantages of these two aspects. The FPN is shown in Figure 3. An effective feature extraction approach is provided for target detection.

Specific algorithms have demonstrated excellent capabilities for detecting small targets, especially those using focus loss functions. A two-stage detection method such as region-based convolutional neural network (Faster R-CNN) first eliminates most of the background by generating candidate regions. Then the precise classification is performed. However, the processing process is relatively slow. It is worth noting that category imbalance can lead to accuracy differences in some algorithms. CE loss is a commonly used evaluation standard, as detailed in equation (12).

$$CE(p,y) = \begin{cases} -\log(p), if \quad y = 1 \\ -\log(1-p), otherwise \end{cases} \tag{12}$$

In equation (12), $p \in [0,1]$ represents the prediction probability. $y \in \{\pm 1\}$ represents the positivity and negativity of the sample. The detailed description of is shown in equation (13).

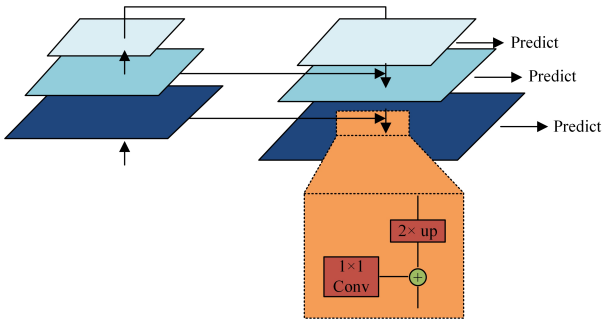

Figure 3: Feature pyramid network

$$p_i = \begin{cases} p, & if \quad y = 1 \\ 1 - p, otherwise \end{cases} \tag{13}$$

To address the type imbalance, the conventional strategy is to introduce a weight coefficient $a \in [0, 1]$. It is also the fundamental part of the focusing loss function, as shown in (14).

$$CE(p, y) = CE(p_t) = -\log p_t \tag{14}$$

When using focus loss for training, if the detector misjudges the training data sample, the p_t value will be very close to 0. For samples with easy classification, the p_t value will be close to 1. The debugging coefficient will be close to 0. The network structure of R-Net is shown in Figure 4.

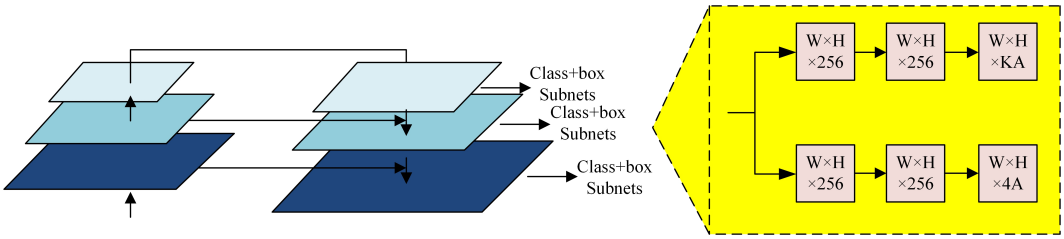

Figure 4: Network structure of R-Net

The R-Net structure utilizes a FPN as its core, supplemented by two task sub-networks. The candidate region generation in this method is similar to the anchor points in RPN networks. Each layer of feature map has 9 anchor points associated with it, based on three sizes and three aspect ratios. This network forms a feature pyramid on the $P_3 \sim P_7 - layer$. With the help of FPN structure and unique focus loss function, R-Net exhibits excellent detection performance on small and medium-sized targets, while maintaining high accuracy for large targets. This provides a powerful tool for defect and fault diagnosis and location on transmission lines.

3.3 Transmission Line Feature Pyramid Network Based on D-Net

The severe regional conditions, climate change, and different equipment qualities encountered have led to various types and characteristics of power transmission channels. The difficulties mentioned above impede the accuracy and precision of conventional skill property extraction. As a result, the technology has been modified to suit the unique situation of power transmission lines. This includes optimizing the size of each feature map, the various sliding windows of the FPN, as well as the predetermined three scales and three aspect ratios. Anchors are densely generated and mapped to their regions on the original map. The set values are shown in equation (15).

$$\begin{cases} \left\{2^0, 2^{1/3}, 2^{2/3}\right\} \\ \{1:2, 1:1, 2:1\} \end{cases} \tag{15}$$

To improve adaptation to the target, the strategy for generating anchors has been enhanced. Traditional methods rely on prior knowledge to design anchors, but this approach may not always be suitable for all objectives. To solve this problem, the K-means++algorithm is combined to cluster the target boxes in the dataset to obtain more accurate anchor size. The K-means algorithm first sets K clusters and randomly selects K data points as cluster centers in the dataset. The specific process is shown in Figure 5.

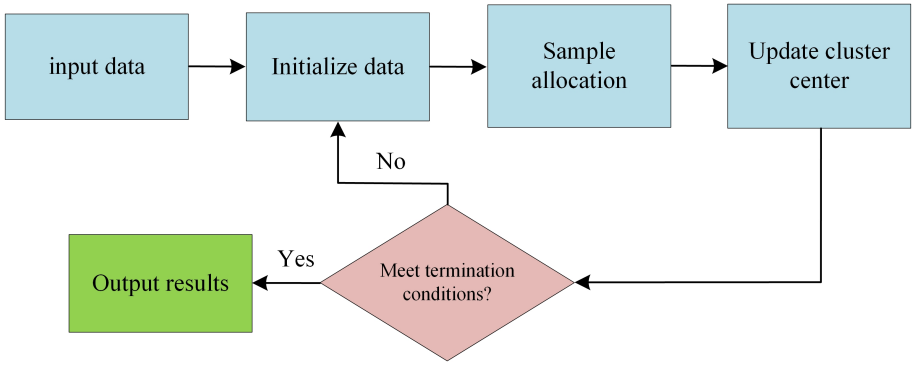

Figure 5: K-means algorithm flowchart

However, the traditional K-means algorithm may produce significant errors in the results if the position of the cluster center is not selected properly. To address this issue, the K-means++ algorithm is developed. This method first selects a center, and then selects the point farthest from this center as the next center. The process is repeated until K centers are selected. The obtained anchor points can better match targets of various sizes, thereby improving recognition accuracy. Anchor generation is achieved by embedding a region proposal network into a FPN. Each feature layer generates multiple anchors with different sizes and aspect ratios [18, 19, 20]. The loss function of R-Net is also adjusted accordingly. The specific process of the K-means++ algorithm is shown in Figure 6. Transmission

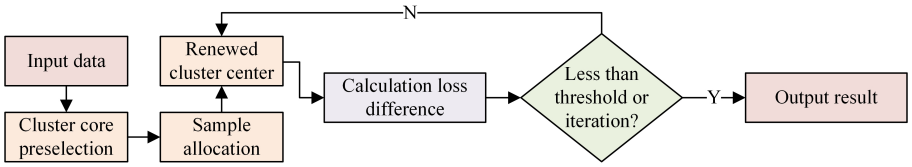

Figure 6: K-means++ algorithm flowchart

lines have numerous defects due to geographical and equipment factors. Traditional algorithms are difficult to extract accurate features, so the algorithm is adjusted. The R-Net is converted to D-Net to adapt to the transmission line environment. The structure of D-Net is efficient and straightforward. It combines the multi-scale feature extraction ability of R-Net, which reduces the number of parameters and computational complexity of the network. This improvement enhances operational efficiency and better adapts to multi-scale defects caused by geographical and equipment factors in the transmission line environment. Experiments have shown that this adjustment improves speed and accuracy. Deep neural networks, as the core of object detection, typically rely on network depth to fit parameters [21]. For example, residual networks and GoogLeNet can improve performance by adjusting network depth and width. However, increasing network complexity can lead to a decrease in training speed and accuracy [22]. A concise network structure can avoid overfitting, accelerate training, and improve accuracy. Therefore, the D-Net is adopted as the core network. The structure is shown in Figure 7. Unlike traditional networks, it strengthens inter layer connections and provides more information flow channels.

The D-Net network consists of multiple D-Net blocks, as shown in Figure 7. The growth rate $K = 4$ represents the number of channels output per layer. The input layer receives the feature map of $N \times N \times C$, and then passes through the bottleneck layer, BN, ReLU, and 3×3 convolutional layer to reach the output layer, generating the feature map of $N \times N \times 4$ [23]. The output of each layer is

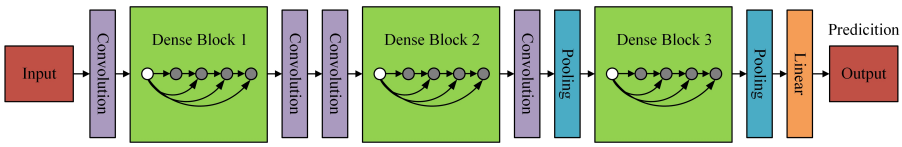

Figure 7: D-Net network structure diagram

concatenated with the input of the previous layer to obtain more channel feature maps. This process is repeated in five layers. The final output is $N \times N \times 4$.

$$x_l = H_i([x_0, x_1, ..., x_{l-1}]) \tag{16}$$

In equation (16), $[x_0, x_1, ..., x_{l-1}]$ is the concatenation result of feature maps between the current layer and all previous layers. H_i represents a series of operations, including BN layer, ReLU activation function, and 3×3 convolutional layer. This design ensures the deep transmission of information in the network and enhances the feature reuse. The experimental environment utilizes the Ubuntu LTS operating system and Python programming language, along with Tensorflow, OpenCV, and other tools [24]. The network initialization for the experiment is based on the parameters of the MS COCO training set. All parameters for the ResNet and DenseNet networks are initialized with a Gaussian distribution with a mean of 0 and variance [25]. The experimental setup involves using the stochastic gradient descent method in a single GPU environment to optimize the loss function in the training data. The initial learning rate is set at 0.01 and is reduced to 10% for further training after specific iterations (50,000 and 70,000 rounds). A total of 40 epochs are trained, with each epoch containing 5,300 iterations, one image per iteration. The weight attenuation coefficient is set to 0.0001 and momentum to 0.9. For focus loss, alpha is set to 0.25 and gamma is set to 2. To address focus loss, the values of alpha and gamma are set to 0.25 and 2, respectively. The initialization process for ResNet101 and F-RCNN networks is also based on a Gaussian distribution, but the learning rate is adjusted differently, only being reduced at the 50th round. During F-RCNN training, each batch processes 256 images, and a total of 70,000 batches are trained. YOLO-v3 initialization follows a similar Gaussian distribution rule. Unlike other models, YOLO-v3 maintains a constant learning rate throughout the training process, training a total of 80,000 batches, each processing 64 images. It has a weight attenuation coefficient of 0.0005 and a momentum of 0.9. To improve the accuracy of fault diagnosis and location in transmission lines, 5840 high-resolution images are collected using unmanned aerial vehicles. The images cover four main defect types: grounding wires, insulators, fittings, and transmission towers. The defects of the tower foundation are also classified as transmission tower defects due to the small amount of data. In total, these images cover over 10000 faulty targets. After annotation, the data is converted into P-VOC format and an XML file is generated containing defect categories and coordinates. A total of 5240 images are used for network training, while 603 images are used for performance evaluation.

4 Result and discussion

The deep learning method is utilized to analyze and diagnose faults in transmission lines. The scheme demonstrates significant superiority in detecting various types of defects, particularly in terms of overall mean average precision (MAP), where the MAP value is reached 0.64, a 1.30% increased from the previous value. The study reveals that in various defect subcategories, such as guide wire defects, the detection accuracy increased by 2.40%, while for tower defects, the increase is only 0.49%, but this result is still significant because it includes irregular defects such as bird's nests. Additionally, the R-Net using the DenseNet121 skeleton has also achieved an overall improvement in detection accuracy, reaching an increase of 1.25%. Significant advancements have been achieved in identifying defects in fittings and guide wires. R-Net, in comparison to other models like F-RCNN and YOLO-v3, not only has a smaller parameter scale but also exhibits superior detection accuracy. For instance, R-Net's MAP outperforms YOLO-v3 by 15.58 percent and F-RCNN by 2.45 percent.

4.1 Training Effects of R-Net on Transmission Line Faults

To ensure network accuracy, the study uses K=12 as the number of anchor boxes. Additionally, to avoid increased computation time resulting from a higher K value, all anchor boxes below a threshold of 0.2 are filtered out. The initial learning rate is set to 0.01, with 5000 iterations, a batch size of 1, weight decay of 0.0001, momentum of 0.9, and focus loss of 2, 0.25. To verify the effectiveness of the new anchor box generation strategy, the performance of the R-Net algorithm before and after improvement is compared. The changes in losses during the training process are shown in Figure 8.

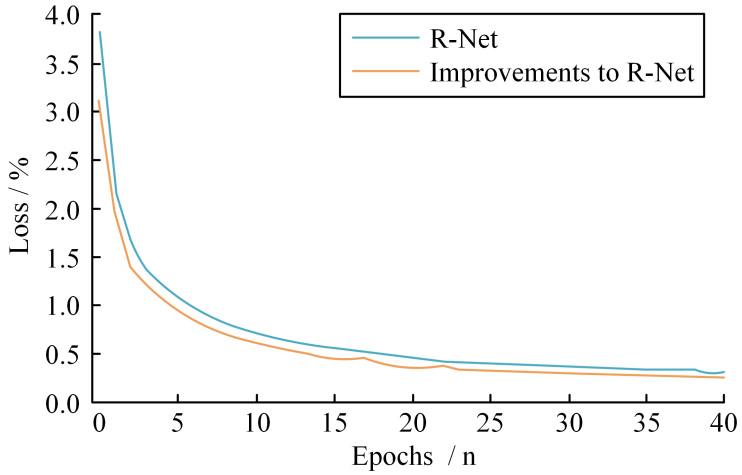

Figure 8: R-Net training loss changes

In Figure 7, the optimized R-Net exhibits significantly lower losses in the initial training phase compared to traditional R-Net. After 40 rounds of training, the loss is 0.46%, which is 0.05% lower than that of traditional R-Net, indicating better stability. This improvement lies in the use of parameters from the MS COCO training set to initialize the anchor box. Based on the optimization, the network has strong object detection capabilities in the early stages, resulting in higher adaptability to targets. In the next 40 iterations, the improved R-Net algorithm continues to exhibit low loss rates. The performance of traditional R-Net and improved R-Net on the test set is shown in Figure 9.

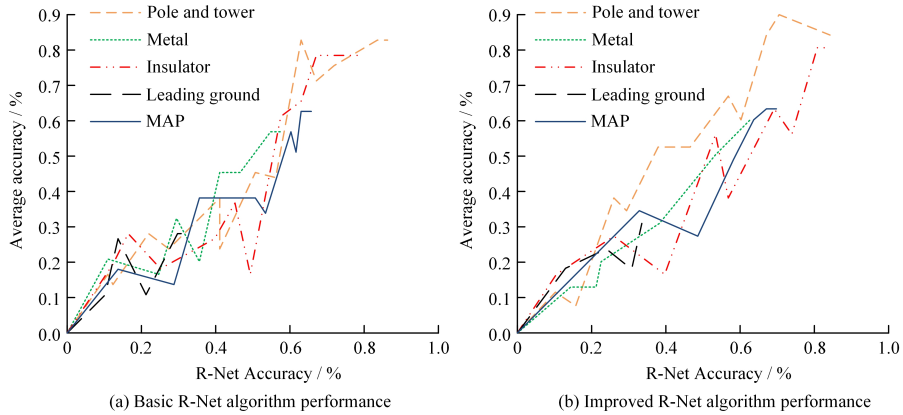

Figure 9: R-Net and improved R-Net algorithm performance

According to Figure 8, the improved R-Net has progress in various defect types. The overall MAP reaches 0.64%, an increase of 1.30%, significantly higher than the traditional R-net ($P<0.05$). The recognition accuracy for metal and insulator are 0.61% and 0.82%, respectively, both higher than the traditional R-Net. For specific minor defects, the accuracy of ground wire defects increases by 2.40%. The accuracy of tower defect increases by 0.49%, with a relatively small increase, which may be due to the irregular shape of such defects, such as bird nests. It is difficult to significantly improve the recognition effect by using the anchor box method. After optimization, the network running speed re-

mained at 10-12FPS, which is equivalent to before optimization. Overall, the recognition performance of this algorithm is significantly enhanced by optimizing the anchor box generation strategy. While improving recognition accuracy, it also maintains a high operating speed.

4.2 Analysis Results of Backbone Network Improvement Based on Transmission Line

ResNet101 and DenseNet121 are chosen as the base structures to improve the performance of R-Net. The backbone network training and testing performance of R-Net optimized with these two different infrastructures are compared to demonstrate the effectiveness of D-Net in enhancing object detection. The difference in the loss curve between the two is shown in Figure 10.

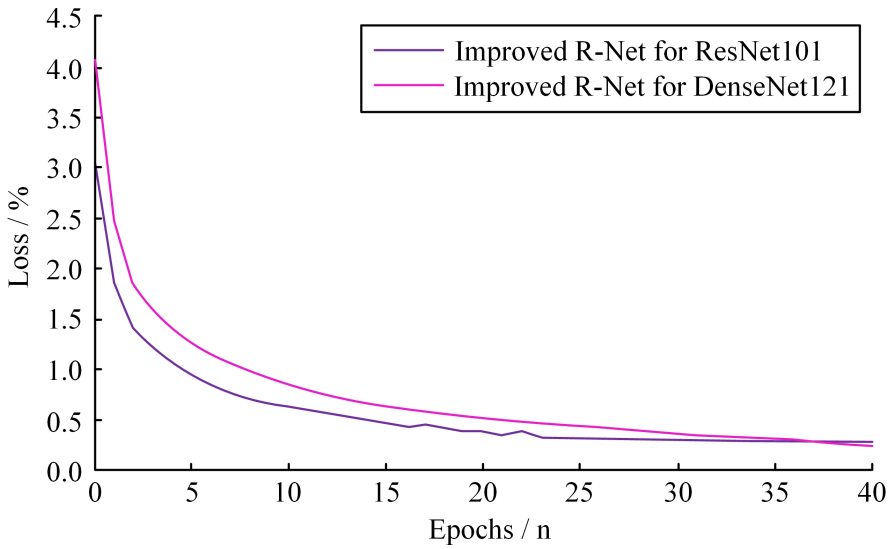

Figure 10: R-Net and D-Net loss curves for different backbone networks

In Figure 9, R-Net with DenseNet121 as the backbone network has a higher loss value than R-Net based on ResNet101 in the initial stage due to the lack of transfer learning. When the iteration exceeded 36 rounds, the version loss value based on DenseNet121 has decreased and exceeded the model based on ResNet101. After deep training, R-Net with DenseNet121 as the backbone network has better adaptability to data. The MAP performance of the two in different defect classifications is shown in Table 1.

Table 1: Comparison of R-Net performance parameters for different types of network optimization

/	Improved R-Net	
Backbone network	ResNet101	DenseNet121
Parameter quantity	56M	17M
The average accuracy of tower detection AP	0.8338	0.8310
The average accuracy of hardware detection AP	0.6029	0.6245
The average accuracy of insulator detection AP	0.8004	0.8038
The average accuracy of ground wire detection AP	0.3130	0.3390
MAP	0.6370	0.6490
FPS	11.5	10.5

Table 1 shows that although R-Net based on DenseNet121 requires only 17M parameters, the MAP reaches 0.6502, which is approximately 1.25% higher than the initial network. In terms of tower defects, R-Net based on DenseNet121 is slightly inferior to the original network, with a decrease of 0.0030%. However, in terms of hardware and ground wire defects, it increases by 2.16% and 2.60%, respectively, enhancing the overall detection accuracy. R-Net, based on DenseNet121, enhances inter layer connectivity and a more complex structure. Although the parameters decreased, the computational requirements increased, resulting in a decrease in FPS to 10.5FPS, lower than the initial model. In summary, the overall defect classification performance of R-Net based on DenseNet121 is

good. However, in practical applications, it is recommended to increase the training depth to improve the network's adaptability and stability. Figure 11 shows the R-Net defect fault detection results optimized based on DenseNet121.

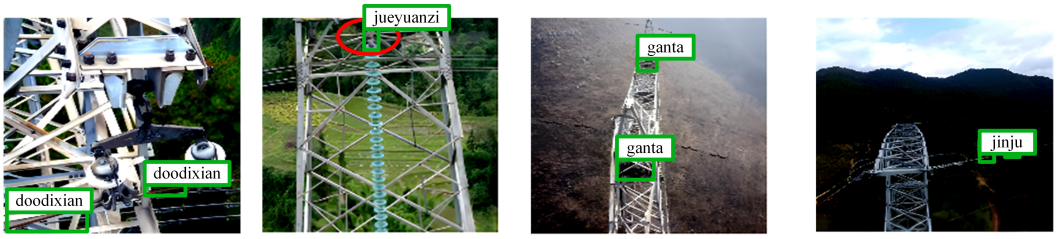

(a) Guide ground fault detection (b) Insulator defect fault detection (c) Tower defect fault detection (d) Hardware defect fault detection

Figure 11: Detection results of four types of transmission line defects

4.3 Comparative Analysis of Different Algorithms Based on Transmission Line Faults

To evaluate the recognition ability of transmission line defect faults, the improved R-Net is compared with different algorithms, including traditional F-RCNN and the third version of YOLO (YOLO-v3). The relevant comparison results are shown in Figure 12.

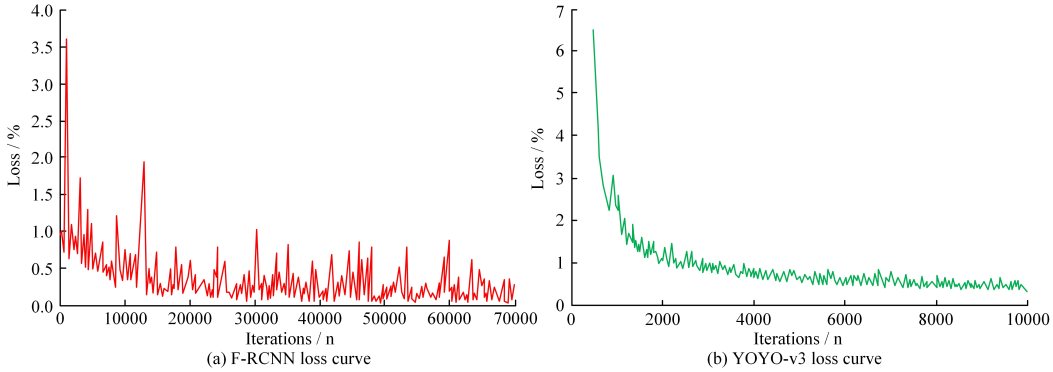

(a) F-RCNN loss curve (b) YOYO-v3 loss curve

Figure 12: F-RCNN and YOLO-v3 loss curves

As the iterations increased, the loss values of each algorithm showed a downward trend. However, different algorithms had different loss scales due to their specific loss calculation methods. Thus, evaluating the matching ability of various algorithms for transmission line defects based solely on these values is challenging. F-RCNN processed 256 images per iteration, resulting in significant fluctuations in the loss function. On the other hand, YOLO-v3 processes 65 images per iteration, resulting in relatively mild oscillations. However, the region recommendation network and target classification network in the F-RCNN algorithm are relatively complex, which may affect real-time performance and efficiency. Additionally, YOLO-v3 may have difficulty accurately detecting small or complex defects. In comparison, the optimized R-Net processes one image at a time, resulting in relatively small oscillations. From the overall number of training iterations, F-RCNN requires approximately 2.6M images, approximately 9900-10000 times. The YOLO-v3 requires approximately 0.39M images, approximately 5500-6000 times. The optimized R-Net based on DenseNet121 requires about 0.25M images and about 39 times. Compared to the YOLO-v3 and YOLO, the optimized R-Net training is more efficient. The test results of optimized R-Net based on F-RCNN, YOLO-v3, and DenseNet121 are shown in Table 2.

In Table 2, the optimized R-Net network has the best average accuracy in identifying common defects in transmission lines, followed by F-RCNN. YOLO-v3 has the weakest performance. In terms of accuracy, the MAP of the optimized R-Net network is 15.58% higher than YOLO-v3, and also exceeds F-RCNN by 2.45%. The R-Net, which is optimized by combining DenseNet121 and FPN,

Table 2: Comparison of different algorithms

/	F-RCNN	YOLO-v3	Improved R-Net
argument	81M	38M	17M
Tower testing AP	0.8049	0.5945	0.8310
Hardware testing AP	0.6084	0.5710	0.6245
Insulator detection AP	0.7985	0.5580	0.8038
Ground cable detection AP	0.2805	0.2500	0.3390
MAP	0.6245	0.4932	0.6490
FPS	4.5	29	10.5

can extract features at different scales and fuse them. This leads to better adjustment of the network parameters and structure, resulting in improved sensitivity and accuracy of the network. In terms of network complexity, F-RCNN has the highest number of parameters, followed by YOLO-v3. The R-Net has the lowest number of parameters, including 81M, 38M, and 17M parameters, respectively. This indicates that R-Net model is relatively streamlined. Considering that YOLO-v3 has an simple algorithm architecture and fewer anchor boxes, the speed could reach 29FPS. The optimized R-Net achieves 10.5FPS.

4.4 Discussion

This paper proposes an improved target detection algorithm designed for transmission line defect detection. The algorithm utilizes CNNs to identify transmission line defects and the optimized K-means algorithm to reshape the size and number of anchors for more accurate identification of small changes. Additionally, a FPN is built in R-Net. The experimental results support this hypothesis and demonstrate the clear benefits of the R-Net optimization scheme across various defect types. The scheme's essence is to modify the anchor frame strategy and enhance the network skeleton, resulting in a substantial improvement in the MAP. A dataset of transmission line defects was constructed, and the R-Net algorithm proposed in this paper was tested against the existing comparison algorithms F-RCNN and YOLO-v3. The experimental results showed several significant findings. Firstly, the accuracy of transmission line defect detection was significantly improved by implementing improvements to R-Net, such as the anchor frame selection mechanism and skeleton network optimization. The improved R-Net was slightly slower than YOLO-v3 in terms of speed, but significantly faster than F-RCNN. In terms of accuracy and recall rate, R-Net demonstrated significant improvement compared to the other two algorithms, indicating a lower miss rate with a lighter model. Additionally, the experiment showed that the detection accuracy and speed are impacted by the depth of the backbone network, even when using the same algorithm model. A deeper network can improve accuracy to some extent, but it can also affect detection speed. Based on the above discussion, this study confirmed the potential of deep learning technology in the field of transmission line fault diagnosis and location. The study also highlighted the significant improvements in detection accuracy and efficiency achieved through improved algorithms. Applying the proposed method to the operation and maintenance of power systems can achieve accurate and rapid fault diagnosis, improving the reliability and stability of transmission networks and enhancing the automation level of power systems. However, challenges in data acquisition and annotation may arise in practical applications, particularly for large-scale transmission line image datasets, which may require significant manpower and time. Customized model training and parameter adjustment are necessary to improve the generalizability of the method for different regions and types of transmission lines. However, this process can be complex and cumbersome. Additionally, the study's treatment of irregular defects is limited and needs to be strengthened. Therefore, future research can utilize data augmentation techniques to expand the training dataset. Targeted data augmentation strategies can also be designed specifically for irregular defects to enhance the ability of R-Net to handle them and improve accuracy and robustness in transmission line fault diagnosis. This research provides new ideas and directions for future research and application of related technologies.

5 Conclusion

This study presents an optimized R-Net algorithm for diagnosing and localizing faults in transmission lines. The proposed algorithm showed significant improvements in accuracy, efficiency, and robustness compared to traditional object detection methods. The optimized R-Net achieved an overall average accuracy of 0.64, outperforming the original network by 1.30%. The improvements were achieved by incorporating techniques such as improved anchor point generation, FPN, and D-Net. The proposed approach demonstrated superior performance in terms of mean average precision and parameter efficiency compared to state-of-the-art algorithms like YOLO-v3 and Faster R-CNN. This study's practical value lied in its potential to improve the reliability, safety, and efficiency of power system operation and maintenance by enabling timely and accurate fault diagnosis and localization.

However, the study has limitations, particularly in dealing with irregular defects, which require further investigation. Future research should focus on improving the algorithm's robustness and generalizability, as well as exploring its integration with other sensing and monitoring technologies. The advancement of transmission line fault diagnosis and localization can be improved through the development of online learning and adaptation mechanisms, as well as multi-task and multi-modal fault diagnosis frameworks.

In conclusion, this study contributes significantly to the field of power system operation and maintenance by proposing an optimized R-Net algorithm for transmission line fault diagnosis and localization. The proposed approach has the potential to improve the stability, security, and efficiency of transmission networks, thereby contributing to the reliable and sustainable operation of modern power systems. Further research and development can lead to a more intelligent, resilient, and secure energy infrastructure by integrating deep learning techniques with power system monitoring and control.

References

[1] Guo, Y.; Mustafaoglu, Z. & Koundal, D. (2022). Spam detection using bidirectional transformers and machine learning classifier algorithms, *Journal of Computational and Cognitive Engineering*, 2(1), 5-9. https://doi.org/10.47852/bonviewJCCE2202192

[2] Jia, Y.; Shang, L.; Nan, J.; Hu, G. & Fang, Z. (2022). CFD analysis of fluid-dynamic and heat transfer effects generated by a fixed electricity transmission line interacting with an external wind, *Fluid Mechanics and Material Processing*, 18(2), 329-344. https://doi.org/10.32604/fdmp.2022.017734

[3] Karimi, S.; Dawson, L.; Musilek, P. & Knight, M. (2022). Forecast of transmission line clearance using quantile regression-based weather forecasts, In *IET Generation, Transmission & Distribution*, 16(8), 1639-1647. https://doi.org/10.1049/gtd2.12390

[4] Rajesh, P.; Kannan, R. & Vishnupriyan, J. (2022). Optimally detecting and classifying the transmission line fault in power system using hybrid technique, *ISA Transactions*, 130(3), 253-264. https://doi.org/10.1016/j.isatra.2022.03.017

[5] Fang, B.; Jiang, M. & Shen, J. (2022). Deep generative inpainting with comparative sample augmentation, *Journal of Computational and Cognitive Engineering*, 1(4), 174-180. https://doi.org/10.47852/bonviewJCCE2202319

[6] Goughari, R. S.; Shahbazzadeh, M. J. & Eslami, M. (2020). Detecting faults in VSC-HVDC systems by deep learning and K-means, *Recent Advances in Electrical & Electronic Engineering (Formerly Recent Patents on Electrical & Electronic Engineering)*, 14(4), 515-524. https://doi.org/10.2174/2352096513999201105155206

[7] Fu, Y.; Guo, X.; Mi, Y.; Yuan, M.; Ge, X.; Su, X. & Li, Z. (2021). The distributed economic dispatch of smart grid based on deep reinforcement learning, *IET Generation Transmission & Distribution*, 15(18), 2645-2658. https://doi.org/10.1049/gtd2.12206

[8] Tong, H.; Qiu, R. C.; Zhang, D.; Yang, H.; Ding, Q. & Shi, X. (2021). Detection and classification of transmission line transient faults based on graph convolutional neural network, *CSEE Journal of Power and Energy Systems*, 7(3), 456-471. https://doi.org/10.17775/CSEEJPES.2020.04970

[9] Athamneh, A. A.; Alqudah, A. M. & Aqeil, R. F. (2021). Line voltage-based distance relay using a multistage convolutional neural network classifier, *International Review of Electrical Engineering*, 16(6), 553-565. https://doi.org/10.15866/iree.v16i6.20962

[10] Tan, J. (2021). Automatic insulator detection for power line using aerial images powered by convolutional neural networks, *Journal of Physics: Conference Series*, 1748(4), 1742-6596. https://doi.org/10.1088/1742-6596/1748/4/042012

[11] Mohammadi, S. F.; Mohsen, A. S.; Mengchu, Z. & Abusorrah, A. (2023). Application of machine learning methods in fault detection and classification of power transmission lines: a survey, *Artificial Intelligence Review: An International Science and Engineering Journal*, 56(7), 5799-5836. https://doi.org/10.1007/s10462-022-10296-0

[12] Shakiba, F. M.; Shojaee, M.; Azizi, S. M. & Zhou, M. (2022). Generalized fault diagnosis method of transmission lines using transfer learning technique, *Neurocomputing*, 500(8), 556-566. https://doi.org/10.1016/j.neucom.2022.05.022

[13] Azizi, S. M.; Shakiba, F. M. & Zhou, M. (2022). A transfer learning-based method to detect insulator faults of high-voltage transmission lines via aerial images: distinguishing intact and broken insulator images, *IEEE Systems, Man, and Cybernetics Magazine*, 8(4), 15-25. https://doi.org/10.1109/MSMC.2022.3198027

[14] Qiu, Z.; Zhu, X.; Liao, C.; Shi, D.; Kuang, Y.; Li, Y. & Zhang, Y. (2022). Detection of bird species related to transmission line faults based on lightweight convolutional neural network, *IET Generation, Transmission & Distribution*, 16(5), 869-881. https://doi.org/10.1049/gtd2.12333

[15] Gao, M. & Zhang, W. (2021). Power transmission line anomaly detection scheme based on CNN-transformer model, *International Journal of Grid and Utility Computing*, 12(4), 388-395. https://doi.org/10.1504/ijguc.2021.119565

[16] Nimrah, S. & Saifullah, S. (2022). Context-Free Word Importance Scores for Attacking Neural Networks, *Journal of Computational and Cognitive Engineering*, 1(4), 187-192. https://doi.org/10.47852/bonviewJCCE2202406

[17] Yang, Y. & Song, X. (2022). Research on face intelligent perception technology integrating deep learning under different illumination intensities, *Journal of Computational and Cognitive Engineering*, 1(1), 32-36. https://doi.org/10.47852/bonviewJCCE19919

[18] Dehghani, M.; Kavousifard, A.; Dabbaghjamanesh, M. & Avatefipoir, O. (2020). Deep learning based method for false data injection attack detection in AC smart islands, *IET Generation, Transmission & Distribution*, 14(24), 5756-5765. https://doi.org/10.1049/iet-gtd.2020.0391

[19] Liu, Z.; Tan, H. J. & Fan, S. S. (2022). A wide range on-line energy acquisition method for transmission lines based on resonant choke coil, *IET Power Electronics*, 15(11), 1047-1057. https://doi.org/10.1049/pel2.12288

[20] Cheng, Y.; Wan, Y.; Sima, Y.; Zhang, Y.; Hu, S. & Wu, S. (2022). Text Detection of Transformer Based on Deep Learning Algorithm, *Tehnički vjesnik*, 29 (3), 861-866. https://doi.org/10.17559/TV-20211027110610

[21] Sun, H.; Liu, M.; Qing, Z. & Miller, C. (2020). A self-adapting multi-LSTM ensemble regression mode for failure prediction of transmission line network from wireless mesh nodes' data, *Journal of Computational Methods in Sciences and Engineering*, 21(1), 903-911. https://doi.org/10.3233/JCM-204550

[22] Deng, X.; Li, J.; Ma, C.; Wei, K.; Shi, L.; Ding, M. & Chen, W. (2023). Low-latency federated learning with dnn partition in distributed industrial iot networks, *IEEE Journal on Selected Areas in Communications*, 41(3), 755-775. https://doi.org/10.1109/JSAC.2022.329436

[23] Lu, Y.; Wei, G. & Jiao, S. (2022). Soil multitrophic network complexity enhances the link between biodiversity and multifunctionality in agricultural systems, *Global Change Biology*, 28(1), 140-153. https://doi.org/10.1111/gcb.15917

[24] Shi, Y.; Xue, X. D.; Xue, J. Y. & Qu, Y. (2022). Fault Detection in Nuclear Power Plants using Deep Leaning based Image Classification with Imaged Time-series Data., *International Iournal of Computers Communications & Control*, 17(1), 1-31. https://doi.org/10.15837/ijccc.2022.1.4714

[25] Xia, B.; Han, D.; Yin, X.; Gao, N. (2022). RICNN: A ResNet & Inception Convolutional Neural Network for Intrusion Detection of Abnormal Traffic, *Computer Science and Information Systems*, 19(1), 309-326. https://doi.org/10.2298/CSIS210617055X

Cite this paper as:

Zhang, C.M.; Xu, X.Q.; Liu, S.L.; Li, Y.J.; Jiang, J.F. (2024). Fault Diagnosis and Localization of Transmission Lines Based on R-Net Algorithm Optimized by Feature Pyramid Network, *International Journal of Computers Communications & Control*, 19(4), 6608, 2024.
https://doi.org/10.15837/ijccc.2024.4.6608